Stretching exercises – flexibility in dihydrofolate reductase catalysis

Grover Paul Miller and Stephen J Benkovic

As an enzyme, dihydrofolate reductase performs two tasks: transformation of its substrate dihydrofolate or folate to tetrahydrofolate, using NADPH as a cofactor, and regeneration of the enzyme for a subsequent round of catalysis. Studies discussed in this review highlight the role of conformational flexibility in both of these enzymatic functions.

Address: Department of Chemistry, The Pennsylvania State University, 415 Wartik, University Park, PA 16802, USA.

Correspondence: Stephen J Benkovic
E-mail: sjb1@psu.edu

Chemistry & Biology May 1998, **5**:R105–R113
http://biomednet.com/elecref/1074552100500R00105

Introduction

Dihydrofolate reductase (5,6,7,8-tetrahydrofolate: $NADP^+$ oxidoreductase, EC 1.5.1.3; DHFR) is a ubiquitous enzyme necessary for normal cellular metabolism in both eukaryotic and prokaryotic cells. The primary physiological role of DHFR is maintenance of the intracellular levels of tetrahydrofolate, a precursor of cofactors required for the biosynthesis of purines, pyrimidines, and several amino acids. Several antineoplastic and antimicrobial drugs, such as methotrexate, trimethoprim, and pyrimethamine act by inhibiting DHFR. The clinical importance of DHFR has made it a long-standing target for enzymological studies. Because there is now a wealth of crystallographic and solution-structure information and of kinetic and computational analyses about DHFR, it provides a rich framework for examining fundamental issues in enzymic catalysis.

The catalytic cycle for an enzyme demands an ability to transform substrate to product and to regenerate free enzyme. An intriguing question remains as to how an enzyme reconciles the rigid constraints required to form a reactive complex with the necessity to discriminate between substrate and product in order to release the latter. Recent studies on DHFR have highlighted the inherent structural flexibility of the enzyme, both enabling it to form the appropriate Michaelis complex for the chemistry to occur and also to modulate the enzyme's conformations in a ligand-dependent manner so as to tune ligand specificity within the catalytic cycle.

Overview of the DHFR catalytic cycle

The DHFR enzyme from *Escherichia coli* catalyzes the reduction of 7,8-dihydrofolate (H_2F) or folate, albeit slowly, to 5,6,7,8-tetrahydrofolate (H_4F) using nicotinamide adenine dinucleotide phosphate (NADPH) as a cofactor (Figure 1). In this reaction, the pro-*R* hydrogen of NADPH is transferred to the C6 of the pterin substrate with concurrent protonation of the N5 of the substrate [1]. The kinetic mechanism for DHFR shown in Figure 2 correctly predicts the steady-state kinetic parameters and full time-course kinetics, as a function of substrate and cofactor concentrations and pH [2]. There are two key features of this mechanism relevant to our discussion: firstly, the rate of hydride transfer is pH-dependent and characterized by a pK_a of 6.5 and an optimal rate of 950 s^{-1}; and secondly, at neutral pH the steady-state kinetic turnover is limited by product (H_4F) release from the mixed ternary complex, DHFR•NADPH•H_4F. In the kinetically preferred pathway, a rapid hydride transfer within the Michaelis complex (DHFR•NADPH•H_2F) yields the

Figure 1

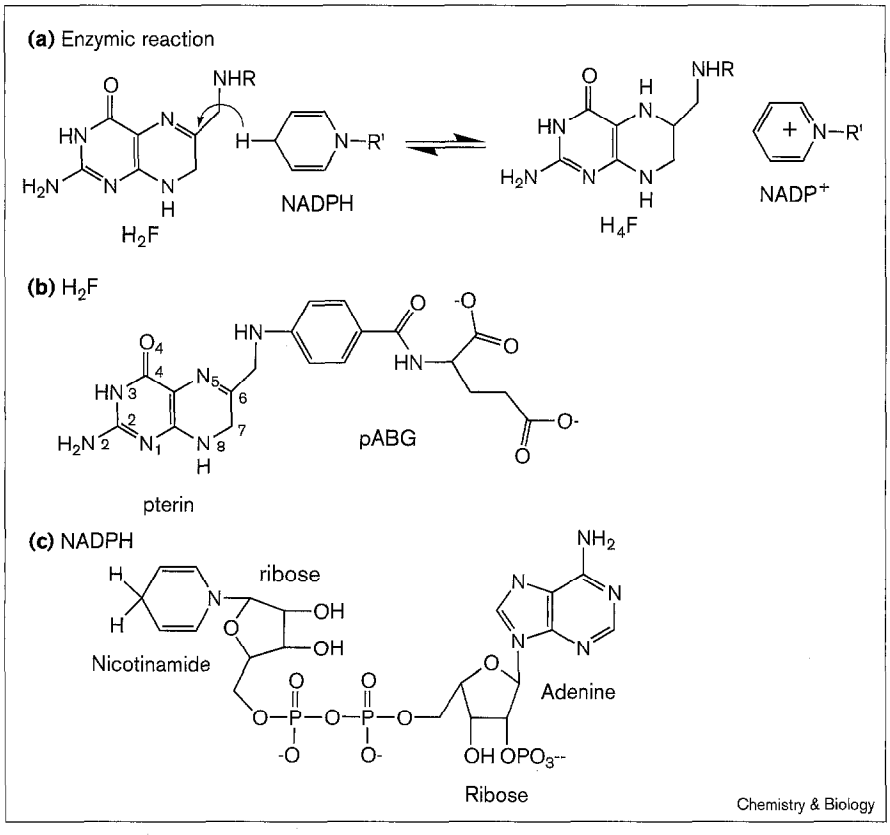

(a) The reaction catalyzed by DHFR. **(b)** The structure of the substrate H_2F. **(c)** The structure of the cofactor NADPH. Folate is an oxidized form of the pterin prior to reduction to 7,8-dihydrofolate and is commonly used to form liganded complexes for analyses. The R and R′ in (a) denote functional groups of H_2F and NADPH, respectively; in (b) pABG denotes the *para*-amino benzoyl group of the H_2F substrate.

ternary product complex, DHFR•$NADP^+$•H_4F, which in turn loses $NADP^+$ to form the binary species, DHFR•H_4F. An additional NADPH molecule required for a subsequent catalytic cycle then binds to form a mixed ternary complex, DHFR•NADPH•H_4F, in which the presence of both ligands results in an antagonistic relationship, or negative cooperativity, so that the off-rates for both ligands are elevated. Because the concentration of NADPH would be

Figure 2

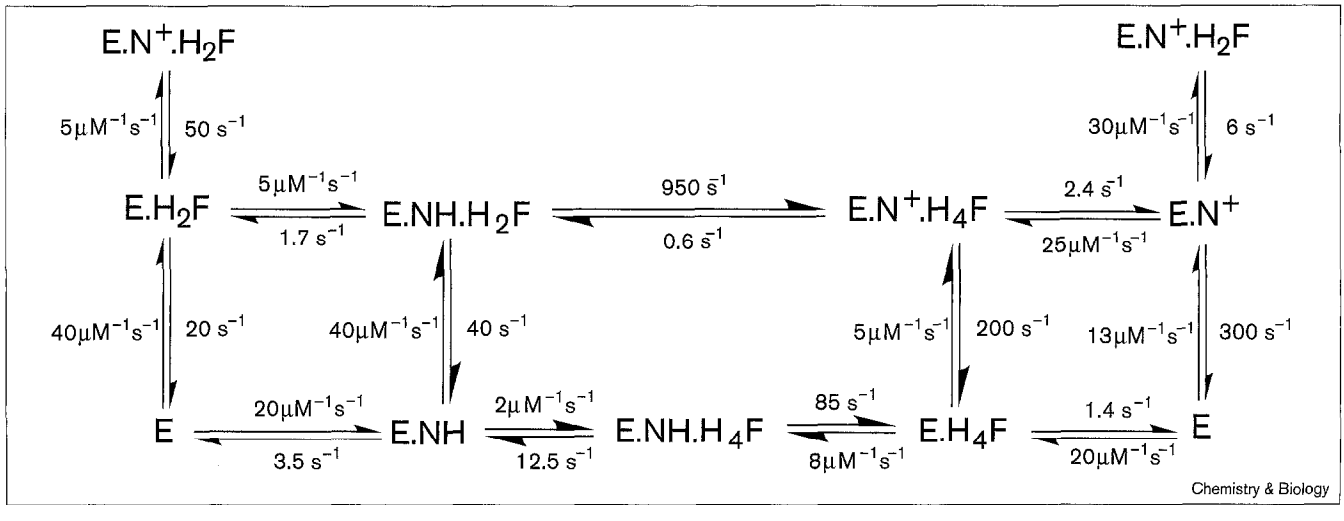

The pH-independent kinetic scheme for catalysis of the H_2F to H_4F reaction by DHFR at 25°C. E, enzyme, NH, NADPH; N^+, $NADP^+$; H_2F, dihydrofolate; H_4F, tetrahydrofolate.

Table 1

Effects of single active-site mutations on ligand binding and hydride transfer.

Active-site mutation	K_D H_2F (μM)	K_D NADPH (μM)	k_{hyd} (s^{-1})	References
Wild type	0.21 ± 0.03	0.33 ± 0.06	950	[3]
H_2F contacts				
Asp27→Asn	NR	0.68 ± 0.05	60	[9–10]
Asp27→Ser	NR	NR	60	[9–10]
Leu28→Phe	0.15 ± 0.06	0.40 ± 0.05	4000	[11]
Leu28→Tyr	0.11 ± 0.02	0.15 ± 0.01	109 ± 5	[12]
Phe31→Val	6.6 ± 0.5	0.22 ± 0.02	120	[13]
Phe31→Tyr	2.6 ± 0.3	0.34 ± 0.03	400	[13]
Leu54→Ile	1.9 ± 0.3	0.30 ± 0.08	31 ± 4	[14]
Leu54→Gly	350 ± 50	0.02 ± 0.01	29 ± 4	[14]
Leu54→Asn	75 ± 15	0.59 ± 0.02	42 ± 8	[14]
Thr113→Val	≥ 12 (45 ± 20)	1.1 ± 0.2	165 ± 5	[15]
NADPH contacts				
Arg44→Leu	0.26 ± 0.02	3.5 ± 0.2	45 ± 3	[16]
His45→Gln	0.33 ± 0.05	2.0 ± 0.2	340 ± 30	[16]
Tyr100→Ile	0.12 ± 0.01	6.5 ± 0.2	35 ± 4	[17]
Tyr100→Gly	0.81 ± 0.09	7.7 ± 0.5	15 ± 1	[17]

NR, not reported.

saturating *in vivo*, the release of H_4F proceeds from the mixed complex to complete the turnover cycle.

The chemical step

Crystallographic and nuclear magnetic resonance (NMR) studies of DHFR plus forms of the substrate and cofactor (including various analogs of these molecules) have revealed the relative orientations of the dihydropterin of H_2F and the nicotinamide ring of NADPH, as well as the location of the sidechain of a mechanistically significant residue, Asp27, of DHFR [3,4]. An important element in optimizing the rate of the hydride-transfer step is the proper alignment of substrate and cofactor. The angle and the distance between hydride donor and acceptor have been shown to be critical determinants of the rate of hydride transfer, both as a result of examining crystal structures of liganded isocitrate dehydrogenase complexes [5] and by *ab initio* calculations for hydride transfer [6]. Using the dihydropyridine-metheniminium cation reaction as a theoretical model for hydride transfer, the optimal C–C bond distance was determined to be 2.6 Å [7]. A model of the expected transition state for the DHFR-catalyzed reaction based on the crystal structure of the ternary DHFR•$NADP^+$•folate complex arrived at a similar distance [8]. The *ab initio* calculation further shows that the energy of activation for hydride transfer is highly sensitive to minor perturbations in the separation distance, which increases by a factor of 0.7–5.0 kcal mol^{-1} for a 0.1–0.3 Å departure from the optimal distance. It is conceivable, therefore, that alterations of key contacts between the reactants and the enzyme might perturb the subtle geometric constraints required for effective hydride transfer.

Although substitutions of a variety of active-site residues that contact the substrate (Leu28, Phe31, Leu54, Thr113) or the cofactor (Arg44, His45, Tyr100) tend to produce marked effects on ligand binding (up to a 10^3-fold increase in the equilibrium dissociation rate constant [K_D]), none of the single mutations is sufficient to reduce the rate of hydride transfer (k_{hyd}) by more than 60-fold (Table 1) [9–17]. The Leu54→Gly mutant protein exhibits an increased K_D for H_2F of 1.7×10^3-fold, but a 30-fold reduction in k_{hyd}; the Tyr100→Gly mutant enzyme shows an increased K_D for NADPH of 20-fold and a comparable 60-fold reduction in k_{hyd}. These findings suggest that there must be significant redundancy and flexibility built into the DHFR active site and the surrounding framework to retain a sufficient population of active enzyme complexes, despite perturbations at key substrate–sidechain contacts.

Another important element revealed by crystallographic studies is the location of Asp27, the only amino acid in the active site that is capable of involvement in protonation of the H_2F 5,6 double bond. In the model for productive substrate binding [8] shown in Figure 3, Asp27 forms hydrogen bonds with Trp22, with Thr113, and with both the 2-amino and 3-NH of the pterin ring. Replacement of Asp27 with asparagine or serine generates mutant forms of DHFR that do not have an acidic proton at the active site and that require preprotonated H_2F for activity [10]. Thr113 hydrogen bonds indirectly to the 2-amino of pterin through a fixed water molecule. Loss of the hydroxyl group, by substitution of Thr113 with valine, results in 200- and 50-fold decreased affinities for H_2F and H_4F, respectively [15]. The rate of hydride transfer by the Thr113→Val mutant enzyme, however, decreases only sixfold, consistent with a minor role for Thr113 in the proton-transfer step. An amphipathic residue, Trp22, coordinates the pterin through hydrogen-bonding another fixed water molecule. When Trp22 is substituted with phenylalanine, substrate affinity

Figure 3

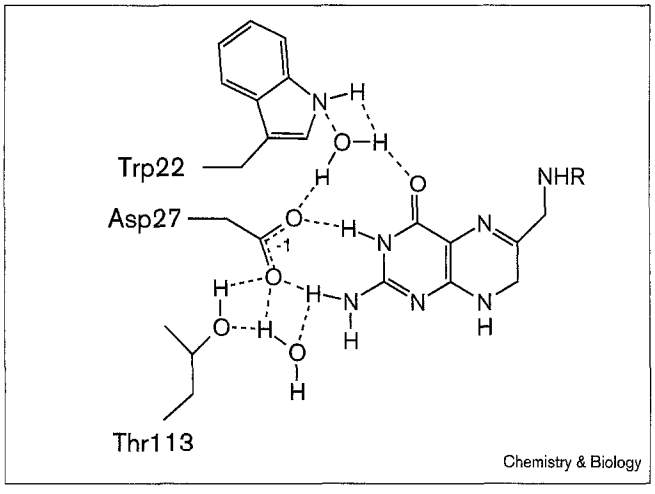

The hydrogen-bond network within the DHFR active site, as derived from the crystal structure of the ternary DHFR•$NADP^+$•folate complex [8].

decreases sixfold, but the hydride transfer rate decreases only threefold, indicating that the hydrogen bonds formed by Trp22 are more important for binding substrate rather than for coordinating and orienting the fixed water molecule involved in the chemical step [18]. Nevertheless, the Asp27 is more than 5 Å from N5 of the pterin ring, so protonation of the pterin N5 appears to occur by an indirect mechanism between donor and acceptor, probably involving an intervening water molecule.

Consistent with crystallographic information [19] and Raman spectroscopic studies [20], a recent computational analysis [21] supports a proposed hydride-transfer mechanism that features a keto–enol tautomerization of the pterin substrate fostered by the low dielectric environment of the DHFR active site (Figure 4). According to this mechanism, the substrate binds initially as a 4-oxo tautomer, forming a dipole-charge interaction with Asp27. To accommodate substrate binding, most of the water molecules are expelled from the active site, thus decreasing the dielectric constant of the environment. The change in the dielectric response shifts the pK_a of Asp27 upwards and serves as the driving force for tautomerization of the pterin ring via a water molecule that transfers a proton to the O4 of pterin, as the pterin N3 proton moves to the carboxylate of Asp27. This coupled rearrangement results in the tautomerization of the pterin ring from the 4-oxo to the 4-hydroxy conformatio, to avoid the unfavorable positioning of a negatively charged carboxylate in a hydrophobic environment, and results in a complex poised for chemical reaction. Synchronized with hydride transfer from the C4 of nicotinamide to the C6 of the pterin is the transfer of a proton from the pterin O4 to the pterin N5, and return of the proton from Asp27 to the pterin N3. As a result of these proton transfers, the newly formed product,

Figure 4

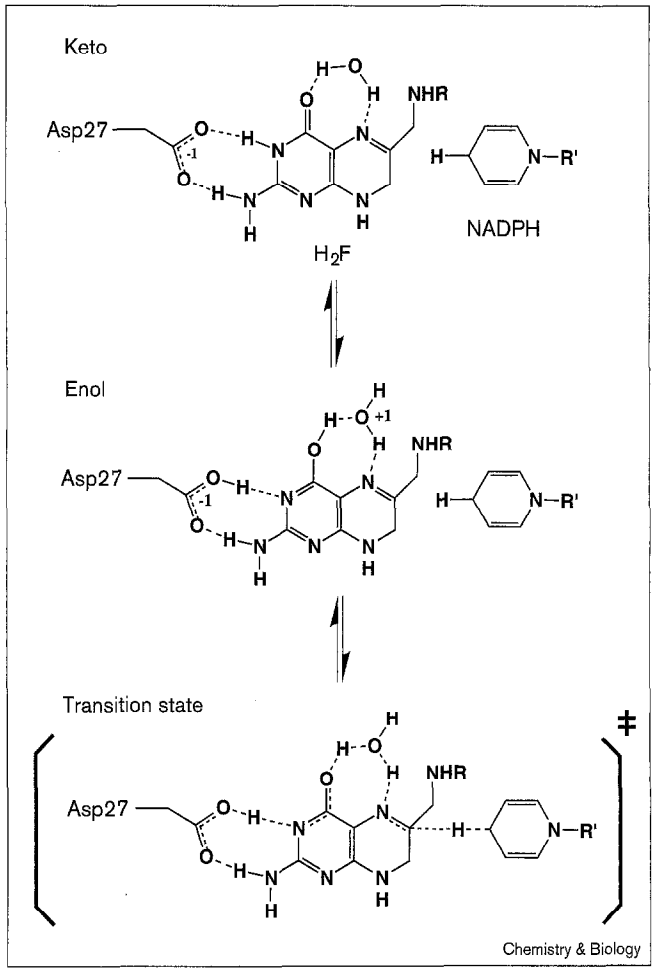

The proposed mechanism of the hydride-transfer reaction. Please see the text for more details.

H_4F, exists in the 4-oxo tautomer form and interacts with the carboxylate of Asp27. The reintroduction of a buried charge in the active-site pocket could explain the increase in the off-rate of product at pHs higher than 6.2 [9].

Thus, an important aspect of the chemical mechanism of DHFR is the dielectric environment of the active site. Stabilizing the charged residues in the active site by increasing solvent accessibility, through substitution of hydrophobic residues with more polar residues, should affect the precision and extent of tautomerization associated with substrate binding and the hydride-transfer rate. These trends are indeed observed experimentally. Substitution of Leu28 by phenylalanine decreases the dielectric response and results in a fourfold higher rate of hydride transfer [11]. Conversely, when another active-site residue, Leu54, is replaced with asparagine or glycine, the rate of hydride transfer drops 30-fold, presumably because a larger, more solvent-accessible active site is created [14]. Moreover, replacement of the central four amino acids of

the Met20 loop (Met16–Ala19) with glycine results in a striking 500-fold decrease in the rate of hydride transfer, probably derived from loss of the loop structure that seals the active site from solvent [22].

Taken together, these results suggest that DHFR catalyzes the reaction through active-site complementarity, forming a ground-state conformation poised for reaction. The binding of substrate and cofactor to the enzyme surface juxtaposes the ligands and aligns them with respect to each other. The low-dielectric environment of the active site induces an electronic reorganization of the reactants to shuffle protons such that they are preorganized in an optimal configuration for catalysis. Finally, the enzyme provides an appropriate environmental backdrop for hydride transfer to occur.

The DHFR scaffold

X-ray crystallographic studies have revealed that the *E. coli* DHFR is a single-domain, monomeric molecule rich in structural elements, including eight-stranded β sheets (strands βA to βH), four α helices, and loop regions connecting these secondary elements ([3] and references therein). The DHFR scaffold is organized into two rigid subdomains, the adenosine-binding subdomain and the loop subdomain. The larger subdomain binds the adenosine portion of NADPH, whereas the smaller subdomain is dominated by three flexible loops: the Met20 loop, the βF–βG loop, and the βG–βH loop. The space between these subdomains forms the active-site cleft, where the cofactor, NADPH, and substrate, H_2F, bind at a 45° angle to each other. The hydride donor (C4 of NADPH) and hydride acceptor (C6 of H_2F) are expected to be held in less than van der Waals contact in the ground state. Access to the active site relies on the conformation of the flexible, largely conserved Met20 loop (residues Ala9–Asn23). As mapped by a series of X-ray crystal structures of complexes thought to mimic turnover complexes, loop movement and rotation between the two subdomains are major elements that underlie the conformational flexibility of DHFR, which serves a critical role in determining the preferred kinetic pathway for the DHFR catalytic cycle.

Modulating ligand binding

Subdomain rotation

Movement of the subdomains modulates the size of the active-site cleft; the largest relative movement is between helix B of the loop subdomain and helix C of the adenosine-binding subdomain. Helices B and C form the two walls of the binding cleft for the *p*-amino benzoyl group (pABG) of substrate. The motion imparted to helices B and C appears to be spread over both subdomains by a shear mechanism [23]. In this model, the overall movement results from the summation of small local motions between closely packed sidechains at the subdomain interface. Specifically, the holoenzyme (DHFR•NADPH) begins the reaction cycle with the subdomains in an open state. Upon

Figure 5

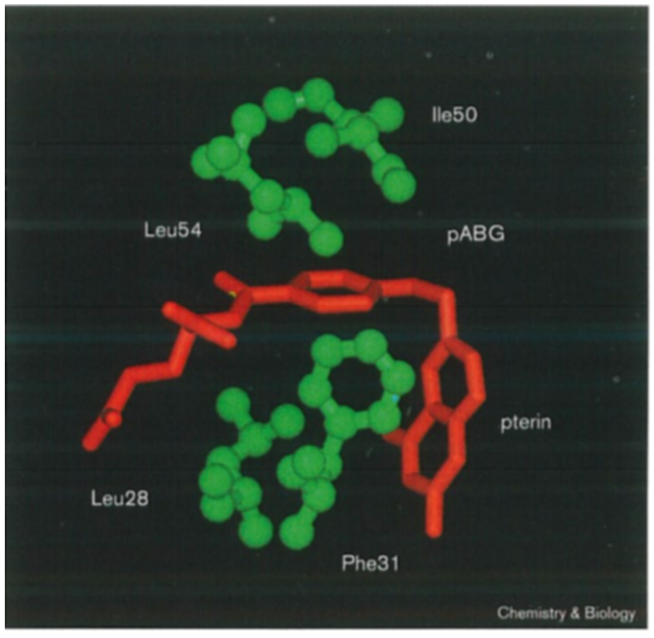

The hydrophobic sidechains that contact the pABG moiety, as determined from the crystal structure of the DHFR•folate complex [3]. Sidechains of the respective residues are green and the pterin molecule is red.

substrate binding, the subdomains rotate closed, sandwiching the pABG through van der Waals contacts from Leu28 and Phe31 in helix B and Ile50 and Leu54 in helix C (Figure 5). These hydrophobic contacts within the active site could be enhanced as the reaction coordinate is traversed. Upon hydride transfer, the reduction of the dihydropterin ring produces a pucker at the C6 of the pterin causing the pABG moiety to shift along the pABG-binding cleft, and for the subdomains to rotate open, as helix B moves to accommodate a shift in the Met20 loop conformational equilibrium. Thus, the van der Waals contacts are disrupted between Leu28 and the pABG moiety. The ability of the subdomains to rotate closed is restored upon $NADP^+$ release, freeing helix C to shift toward the pABG cleft, thus reforming the cluster of van der Waals contacts (Leu28, Phe31, Ile50, Leu54) with the pABG moiety. Upon binding of NADPH, the bridging pyrophosphate draws helix C away from the pABG once more, favoring an open subdomain rotation and loss of H_4F.

An important element in this sequence of conformational changes is the alteration of binding contacts to the pABG moiety. If sidechain interactions are coupled through van der Waals contacts with the pABG moiety, then the contributions of these contacts to the liganded complex would not be additive, despite the fact that the sidechains are on opposite sides of the active site. On the other hand, when enzyme-sidechain–substrate contacts act independently,

the stability of the liganded enzyme complex relies on the sum of all individual binding contacts. In other words, kinetic analyses of site-directed mutants could reveal the discreet steps of the DHFR catalytic cycle involving either an open or closed active-site cleft.

Indeed, the substitution of Leu28 and Leu54 with phenylalanine, both singly and together, and measurement of their effect on the steps in the turnover cycle, explores the individual and collective contributions of the leucine sidechains to liganded DHFR complexes [24]. These two residues are separated by 8 Å and are located in helices B and C. The mutational effects on the kinetics of substrate binding and the forward hydride transfer are generally characterized by nonadditive free energies reflective of sidechain coupling, while the same amino-acid changes have additive effects on the rate of the reverse hydride transfer, the internal equilibrium, and the rate of product dissociation. Hence, extrapolating from the mutations, the ground-state substrate complexes, DHFR•NADPH and DHFR•NADPH•H_2F, have conformations that indicate distal sidechain coupling, whereas the product complexes, DHFR•$NADP^+$•H_4F and DHFR•NADPH•H_4F, and the transition state for hydride transfer, do not.

The simplest explanation for these observations is that the enzyme undergoes a series of conformational changes throughout the catalytic cycle. The substrate and product complexes of wild-type and mutant enzymes have differing conformations that sever or foster the interactions between the sidechains at positions 28 and 54; these different conformations may be ascribed to the open and closed forms noted in the X-ray crystallographic structures. Similar results were obtained for kinetic cycles involving paired substitutions at Phe31 and Ile50 in conjunction with paired Leu28 and Leu54 mutations [12].

The mechanism of subdomain rotation describes two alternate active-site conformations to explain changes in pterin binding observed in the DHFR catalytic cycle. It is conceivable that this movement of the subdomains alters affinity for the cofactor as well. Another important residue in the DHFR active site is Tyr100, which mediates hydrophobic contacts between the nicotinamide ring of the NADPH cofactor and the enzyme. Moreover, the polarizability of the hydroxyl group on the sidechain could contribute to the formation of the transition state. The reduced nicotinamide ring of NADPH is observed to be mostly bound to the enzyme, whereas the oxidized nicotinamide ring of $NADP^+$ remains mainly in the solvent [3,25]. Because the Tyr100–nicotinamide ring contact is more critical in NADPH than in $NADP^+$ binding, the interaction could play a role in differential binding of reduced cofactor over oxidized cofactor that is observed in the DHFR catalytic cycle [2].

As expected, replacement of the tyrosine sidechain with either isoleucine or glycine results in a 20-fold lower affinity for reduced cofactor in the DHFR•NADPH complex without affecting affinity for $NADP^+$ [17]. In fact, the equilibrium dissociation constants for the mutant enzymes are comparable between oxidized and reduced cofactor. The substitution of Tyr100 with isoleucine or glycine also results in a 10- or 20-fold decrease in the rate of hydride transfer, respectively [17]. A decreased rate of hydride transfer is likewise consistent with the previously discussed model for the hydride-transfer reaction in which the proper geometry between the cofactor and substrate is critical during catalysis. The role of the Tyr100 sidechain in orienting the nicotinamide might be compromised by these mutations.

Met20 loop conformations

When the subdomains rotate to accommodate binding of ligands, the Met20 loop adopts one of two ligand-dependent conformations, closed or occluded (this conclusion is based on secondary structure data, interactions with the nicotinamide ring, and hydrogen-bonding patterns with neighboring loops) (Figure 6). The distinction between the Met20 conformations relates to the folding and positioning of residues Glu17–Met20. In the closed conformation observed in substrate/cofactor complexes (DHFR•NADPH and DHFR•NADPH•H_2F), the Glu17–Met20 portion of the Met20 loop forms a short antiparallel sheet and type III′ hairpin turn, which mediates contacts with the nicotinamide ring of cofactor. These interactions are disrupted to attain the occluded Met20 loop conformation observed in product complexes (DHFR•$NADP^+$•H_4F, DHFR•H_4F, and DHFR•NADPH•H_4F). For these liganded species, the central part of the Met20 loop forms a 3_{10} helix, which occludes the binding site for the nicotinamide ring of the cofactor. The stabilization of both Met20 conformers involves hydrogen-bonding interactions with an outer loop, specifically the βF–βG loop in substrate complexes and the βG–βH loop in product complexes. These observations can be viewed in terms of a thermodynamic equilibrium between the closed and occluded conformations that shifts in response to ligand binding.

In the absence of ligand, the central portion of the Met20 loop (residues Met16–Met20) is not observable crystallographically because of disorder in this region [26]. When NADPH binds to DHFR, the Met20 loop adopts the closed conformation in which hydrogen bonds form between the Met20 and βF–βG loops [Gly15(O)–Asp122(N) and Glu17(N)–Asp122(Oε2)]. This closed conformation interacts closely with the cofactor through a hydrogen bond with the carboxamide group of the nicotinamide ring [NADP(N7)–Ile14(O)] and van der Waals contacts between the ribose and backbones of Asn18 and Ala19 and the sidechain of Met20. An important element of cofactor binding, and hence loop closure, is the presence of bound

Figure 6

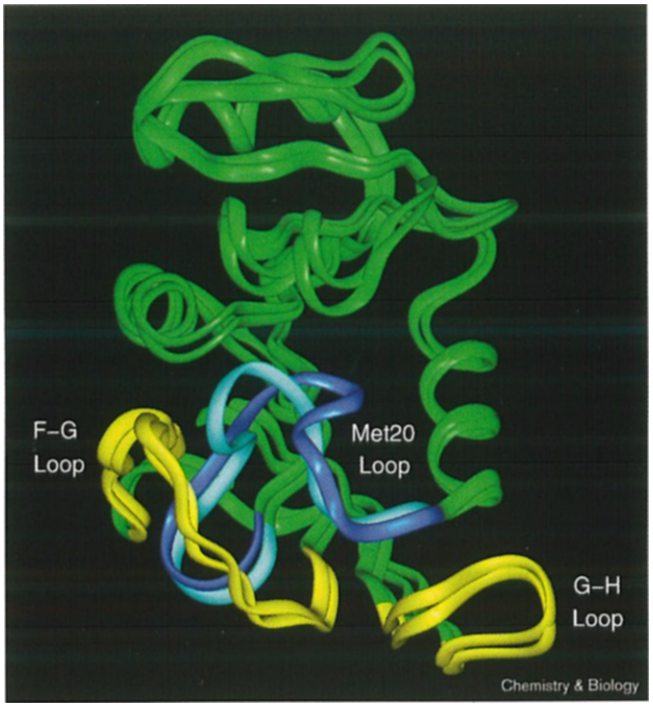

The overlay of the closed and occluded Met20-loop conformations as determined from the crystal structures of the DHFR•NADP$^+$•folate and DHFR•NADP$^+$•ddTHF complexes, respectively [3]. The ddTHF molecule (5,10-dideazatetrahydrofolate) serves as a mimic of the product, H_4F. The scaffold of the protein is shown in green. For the Met20 loop, the closed conformation is lighter blue, whereas the occluded conformation is darker blue. The closed and occluded Met20 loop conformations are stabilized through hydrogen bonds formed with an outer loop, either the βF–βG (F–G) or the βG–βH (G–H) loop, respectively; these outer loops are shown in yellow.

pterin. The formation of a ternary complex juxtaposes the nicotinamide ring and pterin, resulting in favorable van der Waals contacts. When pterin, in this case a folate surrogate for H_2F, binds, the nicotinamide-binding pocket shifts to 100% occupancy, whereas in the absence of bound pterin, the nicotinamide-binding pocket is about 75% occupied. Oxidation of the nicotinamide ring drops the binding pocket occupancy to almost zero for the binary DHFR•NADP$^+$ complex. This aspect of cofactor binding has been observed in both crystallographic and Raman studies [3,25]. Concomitant with cofactor oxidation is the disruption of the hydrogen bonds between the Met20 and βF–βG loops and the formation of strong hydrogen bonds between the Met 20 loop and the βG–βH loop [Asn23(O)–Ser148(N), Asn23(N)–Ser148(Oγ)], as the Met20 loop adopts the occluded conformation for product complexes.

Whereas crystallographic data provide a static window into conformational changes, NMR studies of DHFR describe the dynamic nature of flexible structural elements. A variety of NMR studies have probed the solution structure of DHFR in the absence and presence of its ligands, substrate (folate), cofactor and product. Analysis of the two-dimensional nuclear Overhauser spectra of the apo-enzyme suggests that the Met20 loop exists in an equilibrium between two conformations [27]. In this study, the exchange of Trp22 between two environments serves as an indicator of Met20 loop dynamics. The Met20 active-site loop oscillates at a frequency (35 s^{-1}), similar to the off-rates of the ligands, including product, under steady-state conditions (12 s^{-1}). From the solution structure of the uniformly ^{15}N-labeled DHFR•folate complex, the backbone amides of residues Met16–Ala19 of the Met20 loop and residues Glu120–His124 of the βF–βG loop display structural fluctuations on the nanosecond timescale associated with large amplitudes of motion (S^2 values) [28]. Clearly, these two measurements are on different timescales, but they emphasize the importance of loop movement as a determinant in optimizing the turnover rate of the various complexes in the catalytic cycle.

Kinetic studies have further implicated the conformational and dynamic importance of these active-site loops. When the central portion of the Met20 loop (residues Met16–Ala19) is replaced with glycine, the affinity for substrate and cofactor decreases almost tenfold with a corresponding decrease in the hydride-transfer rate [22]. An indirect approach to addressing the relevance of Met20 loop conformations involves modification of the outer βF–βG and βG–βH loops which, in turn, stabilize the closed and occluded Met20 loop conformations, respectively. In fact, substitution of Gly121 in the βF–βG loop with valine, which would presumably constrain loop flexibility, destabilizes substrate complexes, resulting in a 40-fold loss in NADPH affinity without affecting substrate binding, decreases the rate of hydride transfer 200-fold, and introduces a kinetically significant step for conversion of an initial DHFR′•NADPH•H_2F complex to the reactive ternary Michaelis complex (DHFR•NADPH•H_2F) (the prime denotes a novel ternary species whose formation is observed by fluorescence techniques) [29]. Furthermore, deletion of Gly121 results in the observation of multiple conformational changes to attain the Michaelis complex (DHFR•NADPH•H_2F), so the guiding role of the βF–βG loop in complex formation requires flexibility and appropriate positioning of contacts between the βF–βG and Met20 loops in order to maintain the optimal kinetic sequence and associated rate constants [30].

Whereas these latter studies involve potentially dramatic alterations of loop structure, an attempt to alter the equilibrium of the Met20-loop conformations would provide more valuable insight into the appropriateness of this dynamic loop model. To this end, Asp122 in the βF–βG was substituted with asparagine, serine, and alanine — amino acids with decreasing abilities to hydrogen bond [31]. Because the Asp122 sidechain forms a hydrogen bond with the

Table 2

Summary of conformational changes within the DHFR catalytic cycle [3].

DHFR complex	Active-site cleft	Met20-loop conformation	Relative pterin	Affinity for cofactor
DHFR•NADPH•H_2F	Closed	Closed	High	High
DHFR•$NADP^+$•H_4F	Open	Occluded	High	Low
DHFR•H_4F	Closed	Occluded	High	NA
DHFR•NADPH•H_4F	Open	Occluded	Low	Low
DHFR•NADPH	Open	Closed	NA	High

NA, not applicable.

amide backbone of Glu17 and is observed exclusively in the closed Met20 loop conformation, these mutations would not only destabilize substrate complexes, but would also shift the Met20 loop equilibrium to favor product complexes. Indeed, the sequential substitution of weaker hydrogen bond donors at position 122 results in the gradual favoring of the binary-product complex (DHFR•H_4F) and uncoupling of the negative cooperativity between NADPH and H_4F due to lowered NADPH affinity. Nevertheless, the effects of these mutations are manifest not only on the stability of substrate complexes as predicted by the model, but also on product complexes. For example, the hydride-transfer rates in the forward and reverse directions decrease as a result of these substitutions. Although an equilibrium of the Met20 loop between two conformations is an attractive model, it may be too simplistic a model to describe the dynamic element of the Met20 loop. Interestingly, a significant correlation exists between decreased NADPH binding and the decreased hydride-transfer rates resulting from these mutations, indicating that the interactions of Asp122 are along the reaction coordinate leading to the transition state. These data may explain the strict conservation of a short, acidic sidechain at this position in prokaryotic DHFRs.

Conclusions

Taken together, both subdomain rotation and alternate Met20-loop conformations are key to modulating ligand specificity in the preferred kinetic pathway of DHFR catalysis, as summarized in Table 2. In the Michaelis complex (DHFR•NADPH•H_2F), both the active-site cleft and the Met20 loop are closed resulting in high affinity for reduced cofactor and substrate. Once hydride transfer occurs, the active-site cleft opens and the Met20 loop adopts the occluded conformation. Affinity for the oxidized cofactor is low, such that the binary-product complex (DHFR•H_4F) is favored. Loss of $NADP^+$ closes the active site until NADPH binds to form the mixed ternary complex. In the DHFR•NADPH•H_4F complex, affinity for both ligands is low; but saturating levels of NADPH under steady-state conditions favor the release of product to yield the binary DHFR•NADPH complex, when the Met20 loop again adopts the closed conformation. Binding of substrate then closes the active site for another round of substrate turnover.

The studies discussed in this review highlight the role of flexibility in both the transformation of substrate to product and regeneration of the enzyme. Protein–ligand interactions that appropriately align both substrate and cofactor and provide the necessary environment for hydride transfer to occur are dispersed throughout the Michaelis complex. There are only a few single-site mutations that drastically reduce the rate of hydride transfer, so significant redundancy and flexibility are inherent within the DHFR scaffold, allowing it to retain a sufficient population of active enzyme complexes. In contrast, nearly all amino-acid substitutions affect ligand affinity and often uncouple the preferred kinetic pathway observed in the DHFR catalytic cycle. These effects underscore the sensitivity of the conformational flexibility of the DHFR scaffold-forming liganded complexes. Insights into the molecular basis of this dual flexibility serve to broaden our understanding of the structure–function relationships inherent in nature's catalysts and underscore the intricate choreography between the protein fold and the catalytic cycle.

Acknowledgements

We thank W.R. Cannon for helpful discussions concerning DHFR catalysis. This work was supported in part by NIH Grant GM24129. G.P.M. is the recipient of the Homer F. Braddock College of Science Memorial Scholarship.

References

1. Charlton, P.A., Young, D.W., Birdsall, B., Feeny, J. & Roberts, G.C.K. (1979). Sterochemistry of reduction of folic acid using dihydrofolate reductase. *J. Chem. Soc. Chem. Commun.* 922-924.
2. Fierke, C.A., Johnson, K.A. & Benkovic, S.J. (1987). Construction and evaluation of the kinetic scheme associated with dihydrofolate reductase from *Escherichia coli*. *Biochemistry* **26**, 4085-4092.
3. Sawaya, M.R. & Kraut, J. (1997). Loop and subdomain movements in the mechanism of *Escherichia coli* dihydrofolate reductase: crystallographic evidence. *Biochemistry* **36**, 586-603.
4. Falzone, C.J., Benkovic, S.J. & Wright, P.E. (1990). Partial ^1H assignments of the *Escherichia coli* dihydrofolate reductase complex with folate: Evidence for a unique conformation of bound folate. *Biochemistry* **29**, 9667-9677.
5. Mesecar, A.D., Stoddard, B.L. & Koshland, D.E. (1997). Orbital steering in the catalytic power of enzymes: small structural changes with large catalytic consequences. *Science* **277**, 202-206.
6. Benkovic, S.J., Fierke, C.A. & Naylor, A.M. (1988). Insights into enzyme function from studies on mutants of dihydrofolate reductase. *Science* **239**, 1105-1110.
7. Wu, Y.D. & Houk, K.N. (1987). Theoretical transition structures for hydride transfer to metheniminium ion from methylamine and dihydropyridine. On the nonlinearity of hydride transfers. *J. Am. Chem. Soc.* **109**, 2226-2227.
8. Bystroff, C., Oatley, S.J. & Kraut, J. (1990). Crystal structures of *Escherichia coli* dihydrofolate reductase: the $NADP^+$ holoenzyme and the folate•$NADP^+$ ternary complex. Substrate binding and a model for the transition state. *Biochemistry* **29**, 3263-3277.
9. Appleman, J.R., Beard, W.A., Delcamp, T.J., Prendergast, N.J., Freisheim, J.H. & Blakely, R.L. (1990). Role of aspartate 27 of dihydrofolate reductase from *Escherichia coli* in interconversion of active and inactive enzyme conformers and binding of NADPH. *J. Biol. Chem.* **265**, 2740-2748.

10. Howell, E.E., Villafranca, J.E., Warren, M.S., Oatley, S.J. & Kraut, J. (1986). Functional role of aspartic acid 27 in dihydrofolate reductase revealed by site-directed mutagenesis. *Science* **231**, 1123-1128.
11. Wagner, C.R., Thillet, J. & Benkovic, S.J. (1992). Complementary perturbation of the kinetic mechanism and catalytic effectiveness of dihydrofolate reductase by side-chain interchange. *Biochemistry* **31**, 7834-7840.
12. Huang, Z., Wagner, C.R. & Benkovic, S.J. (1994). Nonadditivity of mutational effects at the folate binding site of *Escherichia coli* dihydrofolate reductase. *Biochemistry* **33**, 11576-11585.
13. Chen, J.-T., Taira, K., Tu, C.P.D. & Benkovic, S.J. (1987). Probing the functional role of phenylalanine-31 of *Escherichia coli* dihydrofolate reductase by site-directed mutagenesis. *Biochemistry* **26**, 4093-4100.
14. Murphy, D.J. & Benkovic, S.J. (1989). Hydrophobic interactions via mutants of *Escherichia coli* dihydrofolate reductase: Separation of binding and catalysis. *Biochemistry* **28**, 3025-3031.
15. Fierke, C.A. & Benkovic, S.J. (1989). Probing the functional role of threonine-113 of *Escherichia coli* dihydrofolate reductase for its effect on turnover efficiency, catalysis, and binding. *Biochemistry* **28**, 478-486.
16. Adams, J., Johnson, K., Matthews, R. & Benkovic, S.J. (1989). Effects of distal point-site mutations on the binding and catalysis of dihydrofolate reductase from *Escherichia coli*. *Biochemistry* **28**, 6611-6618.
17. Adams, J.A., Fierke, C.A. & Benkovic, S.J. (1991). The function of the amino acid residues contacting the nicotinamide ring of NADPH in dihydrofolate reductase from *Escherichia coli*. *Biochemistry* **30**, 11046-11054.
18. Warren, M.S., Brown, K.A., Farnum, M.F., Howell, E.E. & Kraut, J. (1991). Investigation of the functional role of tryptophan 22 in *Escherichia coli* dihydrofolate reductase by site-directed mutagenesis. *Biochemistry* **30**, 11092-11103.
19. Lee, H., Reyes, V.M. & Kraut, J. (1996). Crystal structures of *Escherichia coli* dihydrofolate reductase complexed with 5-formyltetrahydrofolate (folinic acid). in two space groups: evidence for enolization of pteridine O4. *Biochemistry* **35**, 7012-7020.
20. Chen, Y.Q., Kraut, J., Blakely, R.L. & Callender, R. (1994). Determination by Raman spectroscopy of the pKa of N5 of dihydrofolate bound to dihydrofolate reductase: mechanistic implications. *Biochemistry* **33**, 7021-7026.
21. Cannon, W.R., Garrison, B.J. & Benkovic, S.J. (1997). Electrostatic characterization of enzyme complexes: evalution of the mechanism of catalysis of dihydrofolate reductase. *J. Am. Chem. Soc.* **119**, 2386-2395.
22. Li, L., Falzone, C.J., Wright, P.E. & Benkovic, S.J. (1992). Functional role of a mobile loop of *Escherichia coli* dihydrofolate reductase in transition-state stabilization. *Biochemistry* **31**, 7826-7833.
23. Gerstein, M., Lesk, A.M. & Chothia, C. (1994). Structural mechanisms for domain movements in proteins. *Biochemistry* **33**, 6739-6749.
24. Wagner, C.R., Huang, Z., Singleton, S. & Benkovic, S.J.(1995). Molecular basis for nonadditive mutational effects in *Escherichia coli* dihydrofolate reductase. *Biochemistry* **34**, 15671-15680.
25. Zheng, J., Chen, Y.Q. & Callender, R. (1993). A study of the binding of NADP coenzymes to dihydrofolate reductase by Raman difference spectroscopy. *Eur. J. Biochem.* **215**, 9-16.
26. Bystroff, C. & Kraut, J. (1991). Crystal structures of unliganded *Escherichia coli* dihydrofolate reductase: Ligand-induced conformational changes and cooperativity in binding. *Biochemistry* **30**, 2227-2239.
27. Falzone, C.J., Wright, P.E. & Benkovic, S.J. (1994). Dynamics of a flexible loop in dihydrofolate reductase from *Escherichia coli* and its importance for catalysis. *Biochemistry* **33**, 439-442.
28. Epstein, D.M., Benkovic, S.J. & Wright, P.E. (1995). Dynamics of the dihydrofolate reductase-folate compelx: Catalytic sites and regions known to undergo conformational changes exhibit diverse dynamical features. *Biochemistry* **34**, 11037-11048.
29. Cameron, C.E. & Benkovic, S.J. (1997). Evidence for a functional role of the dynamics of glycine 121of *Escherichia coli* dihydrofolate reductase obtained from kinetic analysis of a site-directed mutant. *Biochemistry*, **36**, 15792-15800.
30. Miller, G.P. & Benkovic, S.J. (1998). Deletion of a highly motional residue affects formation of the Michaelis complex for *Escherichia coli* dihydrofolate reductase. *Biochemistry*, in press.
31. Miller, G.P. & Benkovic, S.J. (1988). Strength of a hydrogen bond determines the kinetic pathway in catalysis by *Escherichia coli* dihydrofolate reductase. *Biochemistry*, in press.